Storer, A. C., & Cornish-Bowden, A. (1976) *Biochem. J. 159*, 1–5.
Sufrin, J. R. (1979) in *Transmethylation* (Usdin, E., Borchardt, R. T., & Creveling, C. R., Eds.) pp 27–36, Elsevier/North-Holland, New York.
Tallan, H. H. (1979) *Biochem. Med. 21*, 129–140.
Winter, C. G., & Christensen, H. N. (1964) *J. Biol. Chem. 239*, 872–878.

6-(*p*-Toluidinyl)naphthalene-2-sulfonic Acid as a Fluorescent Probe of Yeast Hexokinase: Conformational States Induced by Sugar and Nucleotide Ligands†

Gordon V. Ohning‡ and Kenneth E. Neet*

ABSTRACT: The fluorescent dye 6-(*p*-toluidinyl)naphthalene-2-sulfonic acid (2,6-TNS) has been shown to be a sensitive and nonperturbing probe of conformational states of yeast hexokinase. The binding of sugar ligands to hexokinase induced conformational states of the enzyme which could be distinguished by monitoring 2,6-TNS fluorescence and correlated well with their behavior during the catalytic reaction. The binding of five-carbon sugar inhibitors such as lyxose induced a conformational state of hexokinase that demonstrated a small quenching of 2,6-TNS fluorescence but an increased ability to bind metal–ligands when compared to free enzyme. The binding of good sugar substrates such as glucose produced a conformational state of hexokinase which demonstrated a large enhancement (37%) of bound 2,6-TNS fluorescence. This glucose-induced conformational state had an increased ability to bind metal–ATP ligands; however, the relative changes in the dissociation constants for the various metal–ATP ligands differ from those observed with hexokinase in the presence of lyxose. Hence, the lyxose-induced conformational state of hexokinase was concluded to be significantly different from the glucose-induced conformational state. The binding of poor sugar substrates such as 5-thioglucose induced a conformational state of hexokinase similar to the conformational state induced by glucose, but with a smaller enhancement of 2,6-TNS fluorescence (15%) and a lesser ability to increase the affinity for metal–ATP ligands. The six-carbon inhibitor with a bulky group on the 2-position, *N*-acetylglucosamine, gave minimal changes in 2,6-TNS fluorescence and effects on metal–nucleotide binding. These conformational states are interpreted in terms of the closure of the cleft between the two domains observed by X-ray crystallography. The binding of AlATP to free hexokinase was not observed at concentrations up to 100 μM, which is consistent with the kinetic properties reported for this metal–ATP ligand. Although both CrATP and AlATP have been reported to produce a slow burst-type transient in the progress curve of hexokinase, only CrATP demonstrated slow changes in 2,6-TNS fluorescence, indicating that the conformational state of hexokinase induced by AlATP is different from the conformational state induced by CrATP.

Yeast hexokinase catalyzes the phosphorylation of certain hexose sugars in the presence of MgATP. The rate at which this reaction proceeds varies among the sugars from good substrates such as glucose to poor substrates such as 5-thioglucose and mannosamine (De Domenech & Sols, 1980; Viola et al., 1980). Metal(III)–ATP ligands act as inhibitors of hexokinase, and several of these ligands cause a slow, burst-type transient in the hexokinase progress curve when added to the assay mixture (Danenberg & Cleland, 1975; Viola et al., 1980). A random mechanism for the hexokinase-catalyzed phosphorylation reaction has been demonstrated (Fromm & Zewe, 1962; Rudolph & Fromm, 1971b; however, a preferred order of substrate addition, with sugar substrates binding prior to metal–nucleotide, has also been reported (Noat et al., 1969; Wilkinson & Rose, 1979; Danenberg & Cleland, 1975). Recent kinetic studies have demonstrated synergism in the binding of MgATP and certain sugar substrates (Viola et al., 1980, 1982). Several investigators have suggested that substrate–hexokinase interactions involve conformational changes in the enzyme. Physical studies of hexokinase structure, including X-ray crystallography (Bennett & Steitz, 1978), X-ray light scattering (McDonald et al., 1979), and intrinsic fluorescence (Zewe et al., 1964; Peters & Neet, 1978), have demonstrated that a large conformational change in hexokinase occurs upon binding glucose. X-ray crystallography suggests that the large conformational change with glucose is a movement of two domains of the enzyme toward each other with glucose situated within the cleft (Bennett & Steitz, 1978); this closure is sterically inhibited by certain six-carbon inhibitors with bulky groups in the 2-carbon position, such as *o*-toluoylglucosamine (Anderson et al., 1978). Furthermore, the binding of xylose to hexokinase crystals induced structural changes that were different from those observed upon binding glucose or *o*-toluoylglucosamine (Anderson & Steitz, 1975). The binding of glucose to yeast hexokinase results in a 12% quenching of intrinsic tryptophan fluorescence (Zewe et al., 1964; Feldman & Kramp, 1978) which is independent of ionic strength (Mayer et al., 1982). Fluorescence titration experiments have shown that glucose enhanced the binding of Cr$(NH_3)_2$ATP and that lyxose, a five-carbon analogue of glucose, quenched the intrinsic fluorescence of yeast hexokinase only after prior addition of Cr$(NH_3)_2$ATP (Peters & Neet, 1978).

† From the Department of Biochemistry, Case Western Reserve University, Cleveland, Ohio 44106. *Received December 30, 1982.* This work supported by Grant AM-12881 from the U.S. Public Health Service. A preliminary report of this work was presented at the 184th National Meeting of the American Chemical Society, Kansas City, MO, Sept 1982.

‡ Predoctoral trainee of the U.S. Public Health Service (National Institutes of Health Grant GM 07250). This work was submitted to Case Western Reserve University in partial fulfillment of the requirements for a Doctor of Philosophy degree (Ohning, 1983).

0006-2960/83/0422-2986$01.50/0

Free ATP has been reported to quench hexokinase fluorescence (Zewe et al., 1964); however, this result must be interpreted with caution due to the report of metal contamination in commercial ATP preparations (Womack & Colowick, 1979).

The conformational changes in hexokinase structure that result from the binding of various sugar and metal–nucleotide ligands have not been fully investigated. In this paper, we report the use of 6-(*p*-toluidinyl)naphthalene-2-sulfonate (2,6-TNS)[1] as a fluorescent probe of hexokinase conformational states in the presence of various sugars and metal–nucleotides. Furthermore, intrinsic tryptophan fluorescence and circular dichroism have been examined as probes of hexokinase conformation. These results are used to bridge between the catalytic studies and the static, crystallographic information available on yeast hexokinase.

Materials and Methods

Hexokinase PII was purified from Red Star yeast (Universal Foods Corp.) by the method of Rustum et al. (1971) with minor modifications. Proteolysis was inhibited by use of both phenylmethanesulfonyl fluoride (PMSF) and diisopropyl fluorophosphate (DFP). Yeast cells were lysed by use of a French press (American Instrument Co.), and a Sephadex G-25 column was used to desalt the ammonium sulfate precipitated protein instead of dialysis. Concentrated fractions were stored at 4 °C in 1 M NaCl, 50 mM succinate, and 1 mM EDTA, pH 5.5, and the specific activities of various preparations ranged from 550 to 650 μmol min^{-1} mg^{-1}. Hexokinase SII was purchased from Sigma Chemical Co. (hexokinase type C-302, lot 120F-80803) and was further purified by use of affinity chromatography by using a Sepharose–*N*-(8-aminooctanoyl)-2-amino-2-deoxy-D-glucopyranose-resin prepared by the method of Holroyde et al. (1976) with the following modifications. 8-Aminooctanoic acid was used instead of 6-aminohexanoic acid, and the deprotection of the *N*-[*N*-(trifluoroacetyl)-8-aminooctanoyl]-2-amino-2-deoxy-D-glucopyranose derivative was performed in 80% piperidine. The final product was coupled to freshly prepared CNBr-activated Sepharose 4B at a concentration of 12 μmol of product/g of gel. The affinity column was equilibrated with 5 mM TEA and 1 mM EDTA, pH 6.5, and hexokinase was dialyzed against this same buffer prior to loading the column. The column was washed with several bed volumes of the same buffer to remove any unbound protein. Hexokinase was eluted by using either a linear gradient developed to 100 mM NaCl, 5 mM TEA, and 1 mM EDTA, pH 7.5, or a stepwise gradient by using 70 mM NaCl, 5 mM TEA, and 1 mM EDTA, pH 7.5. The classification of hexokinase as PII was determined by its ability to form dimers in 100 mM TEA, pH 6.5, as monitored by the techniques of sedimentation velocity ultracentrifugation and reacting enzyme gel filtration. Hexokinase SII did not associate to dimers under these conditions. Both enzymes were shown to be monomers at the concentrations used for the fluorescence assays. Protein concentrations were calculated based on an $E^{1\%}_{280}$ of 9.47 (Colowick, 1973).

Glucose-6-phosphate dehydrogenase (type XXI, from *Leuconostoc mesenteriodes*) was purchased from Sigma Chemical Co. 2,6-TNS (lot 2201LH), 1,8-ANS, and xylose were purchased from Aldrich Chemical Co., Inc. 2,6-ANS, 1,5-DNS, 2,6-MANS, and 4,4′-bis(ANS) were obtained from Molecular Probes, Inc. Terbium chloride was purchased from Alpha Products. All other chemicals were obtained from Sigma Chemical Co. and were the best grade available. CrATP was prepared by the method of De Pamphilis & Cleland (1973).

Fluorescence measurements were conducted on an Amin-co-Bowman spectrophotofluorometer (American Instrument Co.) which had been updated by addition of an off-axis ellipsoidal condensing system and a Ratio II accessory. An excitation slit width of 1 mm was used, resulting in a 5.5-nm band-pass. Excitation and emission spectra were obtained by using a Hewlett-Packard Model 7035B X-Y recorder. All measurements were made with a 3-mm light-path square quartz cell at 25 °C. Relative fluorescence intensities were corrected for background fluorescence and dilution. Corrections for inner-filter effect were performed by the method of Brand & Witholt (1967). All combinations of hexokinase with sugar and metal–ATP ligands were examined for time-dependent changes in fluorescence intensity, with the incident light blocked between measurements to avoid UV denaturation of the protein or fluorescent probe. The method of continuous variation, as described by Job (1928), was used to determine the molar binding ratio of 2,6-TNS to hexokinase. In this method, the concentrations of hexokinase and 2,6-TNS are varied, but the sum of these molar concentrations is held constant. A plot of relative fluorescence vs. mole fraction of enzyme will demonstrate a maximum value at the mole fraction corresponding to the binding ratio. The quantum yield of 2,6-TNS bound to hexokinase was estimated by the comparative method (Chen et al., 1969), using the quantum yield for 2,6-TNS in 60% dioxane [0.17 (McClure & Edelman, 1966)], which has an emission maximum of 454 nm. The fraction of 2,6-TNS bound to hexokinase was calculated by using the dissociation constant determined for this complex and the relative quantum yield for the hexokinase-bound 2,6-TNS estimated by correcting the calculated quantum yield for the fraction of 2,6-TNS bound to the enzyme. Additions of ligands were made from filtered, concentrated stock solutions to minimize dilution of the assay mixture. Metal–ATP ligands (other than CrATP) were prepared by mixing equimolar solutions of ATP and metal chlorides or citrate (for metal-free ATP) in water and allowing these mixtures to stand for 1 h at room temperature prior to use. This method has been shown to prepare AlATP satisfactorily, the slowest of the metal–ATP ligands to form a complex (Womack & Colowick, 1979; Neet et al., 1982). Metal–ATP ligand solutions were used within a day of preparation within their respective solubility limits. Metal–ATP stock solutions were adjusted to pH 6.5 prior to use by slow addition of filtered, concentrated NaOH by using a 5-μL Hamilton syringe with rapid mixing to minimize hydrolysis of the ligand. Additions of all solutions were made with Hamilton syringes from the same stock solutions for replicates, taking care not to aerate the solutions. All fluorescence measurements were performed in 100 mM TEA, pH 6.5, with 10^{-4} M 2,6-TNS and 0.1 mg/mL hexokinase unless otherwise indicated. Dissociation constants were obtained by computer fit to binding curve equations by using a nonlinear, least-squares method of analysis on a Northstar Horizon II microcomputer. Statistical significance of dissociation constants for metal–ATP ligands were assessed by use of Student's *t* test.

Kinetic assays were performed at 25° C in 100 mM TEA with 1 mM citrate in 10-mm cuvettes by using pH and ligand concentrations as indicated. Assays were coupled through glucose-6-phosphate dehydrogenase with 0.5 mM NAD or NADP and monitored at 340 nm. Values of K_m and V_{max} were

[1] Abbreviations: 1,8-ANS, 8-anilinonaphthalene-1-sulfonic acid; 2,6-ANS, 6-anilinonaphthalene-2-sulfonic acid; 1,5-DNS, 5-(dimethylamino)naphthalene-1-sulfonic acid; EDTA, ethylenediaminetetraacetic acid; 2,6-MANS, 6-(*N*-methylanilino)naphthalene-2-sulfonic acid; TEA, triethanolamine; 2,6-TNS, 6-(*p*-toluidinyl)naphthalene-2-sulfonic acid.

obtained by fitting velocity data to the Michaelis–Menten equation by using the computer program described above.

CD spectra were obtained at room temperature on a Jasco Model J-40A automatic recording spectropolarimeter (Japan Spectroscopic Company, Ltd.). Measurements in the far-UV region, 190–240 nm, were performed with solutions containing 50 μg/mL hexokinase SII in a 0.1-cm path-length cell. Measurements in the near-UV and visible region, above 250 nm, were obtained by using a 1.0-cm path-length cell and 250 μg/mL concentrations of hexokinase SII. The mean residue ellipticity was calculated by the method of Alder et al. (1973) with a mean residue molecular weight of 115.

Results

2,6-TNS Fluorescence and Interaction with Hexokinase. A variety of (*N*-arylamino)naphthalenesulfonates were tested as possible fluorescent probes of hexokinase conformation by examining the emission spectra of these compounds in the presence of hexokinase SII by using an excitation wavelength of 366 nm. The probes 1,8-ANS, 2,6-ANS, 1,5-DNS, and 2,6-MANS demonstrated little or no increase in their quantum yields and minimal or no changes in their emission maxima upon addition to hexokinase SII. Addition of saturating (50 mM) glucose did not alter these findings. Hence, these compounds either do not bind to hexokinase, or binding does not significantly alter the local environment of the probe. The addition of bis(ANS) to hexokinase SII resulted in a very large increase in the quantum yield of this probe with a concomitant blue shift in its emission maximum from 543 (in 100 mM TEA, pH 6.5) to 505 nm. Examination of this solution using an excitation wavelength of 295 nm indicated that a substantial quenching of intrinsic tryptophan fluorescence occurred upon binding of bis(ANS). Furthermore, a second fluorescence peak at 505 nm was now present in the emission spectrum, suggesting that energy transfer had occurred from the intrinsic tryptophan residues to the hexokinase-bound bis(ANS). Addition of saturating (50 mM) glucose did not alter the emission spectrum of hexokinase-bound bis(ANS), and consequently, this compound was not useful as a probe of hexokinase conformation.

Addition of 2,6-TNS to hexokinase resulted in substantial alterations of both probe fluorescence and intrinsic tryptophan fluorescence. Examination of 2,6-TNS fluorescence using an excitation wavelength of 366 nm indicated that binding of this probe to hexokinase PII resulted in a 54 nm blue shift in its emission maximum, from the 500 nm observed in water to 446 nm upon binding to the enzyme. An estimated 200-fold increase in the quantum yield of 2,6-TNS upon binding to hexokinase PII was observed, based on a relative quantum yield of 0.18. Alterations in intrinsic tryptophan fluorescence due to the binding of 2,6-TNS were observed by using an excitation wavelength of 295 nm (inset, Figure 1). Addition of 10^{-4} M TNS resulted in a substantial quenching of intrinsic tryptophan fluorescence with a concomitant red shift in the emission maximum from 328 to 343 nm. Furthermore, a second emission peak with an emission maximum of 446 nm was observed. Titration of hexokinase SII with 2,6-TNS resulted in enhancement of the emission at 446 nm with a concomitant quenching of the intrinsic tryptophan fluorescence. This observation provides strong evidence of energy transfer between at least one intrinsic tryptophan residue and the bound 2,6-TNS molecule.

Because of the size of the fluorescent change and the sensitivity to substrate binding, 2,6-TNS appeared to be a useful probe for hexokinase. Fluorescence of 2,6-TNS bound to hexokinase SII was characterized as a function of pH, ionic strength, and KI concentration. Fluorescence of hexokinase-bound 2,6-TNS was measured at pH 8.0 and 5.5 by using an excitation wavelength of 295 nm. These emission spectra were not significantly different from the emission spectrum observed at pH 6.5, in the presence or absence of glucose. The effect of ionic strength on probe fluorescence was examined by titration of 2,6-TNS–hexokinase SII solutions with aliquots of saturated KCl. Titration of up to 420 mM KCl resulted in only a slight quenching of the probe fluorescence. The effect of KI, a collisional quencher of solvent-accessible fluorophores (Lehrer, 1971), on 2,6-TNS fluorescence was examined up to 122 mM by using excitation wavelengths of 295 and 366 nm. Quenching of 2,6-TNS–hexokinase SII fluorescence by KI gave linear Stern–Volmer plots with a slope of 6.3 M^{-1} and was virtually identical at both of these excitation wavelengths. Similar results were obtained when KI was used to quench glucose-enhanced, 2,6-TNS–hexokinase SII fluorescence except that the slope was increased to 10.5 M^{-1}. The increased slope of the Stern–Volmer plot for the glucose-enhanced, 2,6-TNS–hexokinase form indicates that the enzyme-bound probe is more exposed to solvent upon the binding of glucose. Hence, the enhanced fluorescence of hexokinase-bound 2,6-TNS observed upon binding of glucose may involve an increase in the rigidity of the probe as well as changes in hydrophobicity of the probe's local environment. The relative contributions of these two mechanisms in the enhancement of 2,6-TNS fluorescence observed upon binding of sugar ligands has not yet been investigated. Use of concentrations of KI above 122 mM resulted in significant changes in the emission maxima of the intrinsic tryptophan and the hexokinase-bound 2,6-TNS emission peaks.

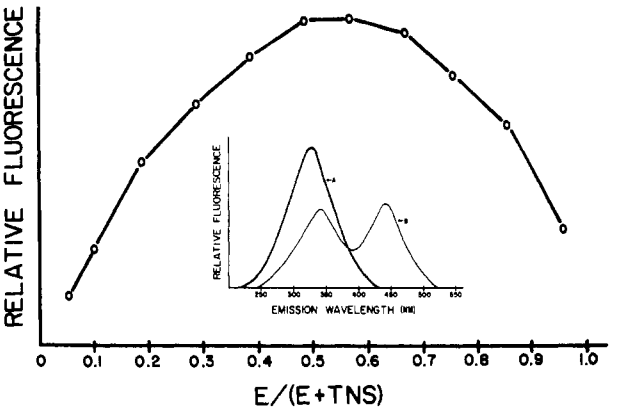

FIGURE 1: Job plot for 2,6-TNS and hexokinase SII. Relative fluorescence is measured as a function of hexokinase SII molar ratio at a constant total (E plus TNS). Data obtained at excitation wavelengths of 295 (shown) and 366 nm were similar. (Inset) Emission spectrum of hexokinase PII in 100 mM TEA, pH 6.5 (A), and in 10^{-4} M 2,6-TNS and 100 mM TEA, pH 6.5 (B). The excitation wavelength was 295 nm. Hexokinase PII concentration was 0.1 mg/mL.

The molar binding ratio was determined by the method of Job (1928), as described above, by monitoring fluorescence emission at 450 nm using an excitation wavelength of either 295 or 366 nm. The maximum-observed fluorescence (Figure 1) occurred at the 0.5 mole fraction value for hexokinase SII at both excitation wavelengths, consistent with a 1:1 molar binding ratio. A dissociation constant of 4.4×10^{-5} M was determined for 2,6-TNS binding to hexokinase SII by titrating a 0.1 mg/mL enzyme solution with the probe. This value was not significantly altered by the presence of 50 mM glucose and 3.3 mM CrATP, or the combination of 5 mM MgATP and 50 mM lyxose. These results indicate that changes in probe fluorescence are not due to changes in the amount of 2,6-TNS that is bound to the enzyme.

Table I: Effect of 2,6-TNS on Hexokinase K_m and V_{max} Values[a]

	2,6-TNS concentration (M)	K_m (mM)	V_{max} (340/min)
	Hexokinase SII at pH 8.0		
vs. ATP	0	0.22 ± 0.03	0.35 ± 0.02
	5×10^{-5}	0.19 ± 0.02	0.32 ± 0.01
	10^{-4}	0.18 ± 0.04	0.26 ± 0.02
vs. glucose	0	0.26 ± 0.01	0.36 ± 0.01
	10^{-4}	0.21 ± 0.01	0.31 ± 0.01
	Hexokinase SII at pH 6.5		
vs. ATP	0	0.27 ± 0.04	0.20 ± 0.01
	10^{-4}	0.21 ± 0.04	0.18 ± 0.01

[a] Effects of 2,6-TNS on the apparent K_m and V_{max} of hexokinase SII at pH 8.0 and pH 6.5. Values obtained by computer fitting of data to Michaelis-Menten equation (see the text).

Kinetic studies were performed to determine if 2,6-TNS was an inhibitor of hexokinase activity. Initial velocities were determined by varying either ATP or glucose at several fixed concentrations of 2,6-TNS. These data were fitted by computer to Michaelis–Menten curves to obtain values for K_m and V_{max}. Apparent inhibition of hexokinase SII activity was only observed at the highest concentration of 2,6-TNS (Table I). Since 2,6-TNS absorbs strongly at the wavelength used for the kinetic assays and high absorbancy of assay solutions has been implicated as an artifact in the apparent inhibition of enzymatic reactions (Cavalieri & Sable, 1974), Dixon plots were obtained for 2,6-TNS vs. glucose or MgATP at pH 8.0 and 6.5 and were consistent with 2,6-TNS having minimal effect on hexokinase SII activity. These kinetic results and the lack of effect of substrates on the dissociation constant of 2,6-TNS clearly indicate that the fluorophore is not binding at the active site of the enzyme.

Since the commercially available enzyme, hexokinase SII, is a partially proteolyzed form (Schmidt & Colowick, 1973), a comparison of 2,6-TNS fluorescence with hexokinase PII and hexokinase SII was performed. The emission maximum for 2,6-TNS bound to hexokinase SII was 438 nm, which is (blue) shifted 8 nm from the emission maximum reported above for hexokinase PII, suggesting that removal of the 11 amino acid, N-terminal peptide (Schmidt & Colowick, 1973) has resulted in a slightly more hydrophobic environment (Stryer, 1965) for the probe. The quantum yield of 2,6-TNS (at 450 nm) in the presence of hexokinase SII, hexokinase PII, and a 1:1 mixture of these enzyme forms was similar (within 5%), indicating that these enzyme forms have similar K_d values with respect to 2,6-TNS. The energy-transfer phenomenon observed at an excitation wavelength of 295 nm occurred with both hexokinase PII and hexokinase SII. Because of the similarities of 2,6-TNS fluorescence in the presence of either hexokinase form and due to the availability of the commercial SII form, the majority of the following studies were performed with hexokinase SII. Selected conditions were repeated with hexokinase PII, as indicated.

The fluorescence emission observed at 450 nm, using an excitation wavelength of 295 nm, for the 2,6-TNS–hexokinase PII complex was linear up to (at least) 0.2 mg/mL hexokinase PII. Neither hexokinase PII or hexokinase SII dimerizes over this concentration range under these conditions (T. C. Furman and K. E. Neet, unpublished results; Schultze & Colowick, 1969). Thus, the changes in fluorescence observed are not due to differences in probe fluorescence with monomer and dimer.

2,6-TNS Fluorescence. Sugar Ligands. The energy-transfer phenomenon described for 2,6-TNS was utilized in the examination of the various conformational states of hexokinase since this system is potentially more sensitive to changes in enzyme conformation than examining 2,6-TNS fluorescence alone. Furthermore, the wide separation of the excitation and emission wavelengths minimizes some of the technical difficulties that are frequently encountered in obtaining fluorescence measurements. This approach was first used to examine the conformational states of hexokinase that were induced by the binding of sugar ligands. Maximum changes in 2,6-TNS fluorescence emission were determined by titration of each ligand to concentrations of at least 100 mM. Saturating concentrations of the various sugar ligands led to a variety of changes in 2,6-TNS fluorescence (Table II). The sugar substrates glucose and fructose, which were classified as good substrates, caused the largest enhancement of 2,6-TNS fluorescence. Binding of 5-thioglucose or mannosamine resulted in an enhancement of 2,6-TNS fluorescence emission, but the increase was quantitatively less than the enhancement observed in the presence of good substrates. N-Acetylglucosamine binding to hexokinase SII did not alter 2,6-TNS fluorescence while the binding of lyxose or xylose resulted in a slight quenching of bound 2,6-TNS fluorescence. The importance of the 6-hydroxyl group is demonstrated by comparing the effect of 2-deoxyglucose, which enhances the 2,6-TNS fluorescence almost as well as glucose, to that of 6-deoxyglucose, which has no effect on the bound 2,6-TNS fluorescence. A dissociation constant for glucose binding to hexokinase SII was calculated to be 0.38 ± 0.05 mM which is in good agreement with values reported in the literature (Colowick, 1973; Mayer et al., 1982). Binding of all sugar ligands except lyxose, xylose, and 6-deoxyglucose resulted in a slight red shift in the emission maximum (Table II).

Table II: 2,6-TNS Fluorescence of Sugar–Hexokinase Binary Complexes[a]

	hexokinase PII	hexokinase SII	
ligand	maximum relative fluorescence	maximum relative fluorescence	shift in emission maximum (nm)
glucose	1.38 ± 0.02	1.37 ± 0.01	+8
fructose		1.37 ± 0.01	+8
2-deoxyglucose		1.31 ± 0.02	+5
5-thioglucose	1.15 ± 0.01	1.15 ± 0.00	+6
mannosamine	1.15 ± 0.02	1.05 ± 0.01	+4
N-acetylglucosamine	1.05 ± 0.01	0.99 ± 0.01	+6
6-deoxyglucose		1.01 ± 0.01	none
lyxose	0.97 ± 0.01	0.97 ± 0.00	none
xylose	0.97 ± 0.00	0.97 ± 0.00	none

[a] Maximum fluorescence emission was observed at 450 nm, relative to ligand-free enzyme, upon titration of sugar ligands with 0.1 mg/mL hexokinase SII or PII in 10^{-4} M 2,6-TNS, 100 mM TEA, pH 6.5. Values listed are the average of three replicates. The excitation wavelength was 295 nm.

Several of these sugar ligand titrations were repeated with hexokinase PII (Table II) and were similar to those obtained with hexokinase SII. The binding of glucose resulted in the greatest enhancement of probe fluorescence, and the binding of lyxose and xylose led to a slight quenching of 2,6-TNS fluorescence emission. Minor differences between the two enzymes were also observed. The binding of *N*-acetylglucosamine resulted in a slight enhancement of the 2,6-TNS fluorescence, and the mannosamine-induced enhancement of the probe fluorescence emission was equivalent to the enhancement observed in the presence of 5-thioglucose. Furthermore, the shifts in the emission maximum of the bound 2,6-TNS that were described for hexokinase SII were not

Table III: Effects of Metal-ATP Ligands on 2,6-TNS-Hexokinase SII Fluorescence[a]

condition	K_d (mM)	maximum change in relative fluorescence quenching[b]
MgATP	1.7 ± 0.4	0.48 ± 0.05
+50 mM lyxose	0.44 ± 0.03	0.65 ± 0.02
+50 mM *N*-acetylglucosamine	2.4 ± 0.7	0.57 ± 0.08
citrate-treated ATP	1.1 ± 0.1	0.36 ± 0.01
+50 mM glucose	0.39 ± 0.03	0.78 ± 0.02
+50 mM lyxose	0.37 ± 0.07	0.37 ± 0.02
+50 mM 5-thioglucose	0.53 ± 0.06	0.54 ± 0.02
+50 mM *N*-acetylglucosamine	1.3 ± 0.3	0.39 ± 0.03
AlATP	no change in fluorescence	
+50 mM glucose	0.0058 ± 0.0012	0.63 ± 0.07
+50 mM lyxose	0.013 ± 0.001	0.67 ± 0.02
+50 mM 5-thioglucose	0.044 ± 0.010	0.57 ± 0.06
+50 mM *N*-acetylglucosamine	0.039 ± 0.005	0.46 ± 0.03
CrATP	0.58 ± 0.05	0.64 ± 0.02
+50 mM glucose	0.32 ± 0.04	1.13 ± 0.06[c]
+50 mM lyxose	0.073 ± 0.008	0.75 ± 0.03
+50 mM 5-thioglucose	0.96 ± 0.11	0.89 ± 0.01
+50 mM *N*-acetylglucosamine	1.0 ± 0.2	0.66 ± 0.06

[a] 2,6-TNS fluorescence of (metal-ATP)-hexokinase binary complexes and (metal-ATP)-sugar-hexokinase ternary complexes with hexokinase SII. Values were obtained by computer fitting data to binding curves. Titrations were performed with 0.1 mg/mL hexokinase SII in 10^{-4} M 2,6-TNS and 100 mM TEA, pH 6.5. Quenching of fluorescence emission was observed at 450 nm by using an excitation wavelength of 295 nm. Due to problems with AlATP solubility, the titration of this metal-ATP ligand was limited to a maximum concentration of 0.1 mM. [b] See Table IV. [c] This value is a fitted value but is overestimated by the error in extrapolation in this case since the limit at complete quenching would be 1.0.

observed with hexokinase PII. The glucose-induced enhancement of bound 2,6-TNS fluorescence was also observed at pH 8.0 and 5.5 (data not shown).

2,6-TNS Fluorescence. Metal–ATP Ligands. The binding of metal–ATP ligands to different conformational states of hexokinase was examined by use of the energy-transfer phenomenon. Since the use of these ligands was limited by problems with the solubility of some of these chelates, the changes observed in 2,6-TNS fluorescence upon binding of these ligands to hexokinase could not be determined at saturating concentrations. Hence, titration curves of metal–ATP ligands with several sugar–hexokinase complexes and free enzymes were obtained, and dissociation constants and maximum fluorescent changes were determined by computer fit of these data to binding equations. All sugar ligands were present at saturating concentrations, as determined by the sugar ligand titrations with hexokinase SII (as described above). Four sugar ligands were chosen to represent the various classes: glucose (good substrate), 5-thioglucose (poor substrate), *N*-acetylglucosamine (six-carbon inhibitor), and lyxose (five-carbon inhibitor). The results of these titrations are presented in Table III, and representative binding curves are shown in Figure 2. The binding of metal–ATP ligands to the sugar–hexokinase complexes resulted in significant quenching of 2,6-TNS fluorescence (Table III). The maximum changes in 2,6-TNS fluorescence observed upon addition of the metal–ATP ligands are reported after changes in 2,6-TNS fluorescence due to binding of the sugar ligands to free hexokinase complex are accounted for. For example, the 78% quenching of 2,6-TNS fluorescence of the glucose–hexokinase complex by citrate-treated ATP occurred subsequent to the 37% glucose-induced enhancement of the 2,6-TNS fluorescence of free hexokinase (Table II). Similar results apply for metal–ATP effects on the other sugar–hexokinase complexes.

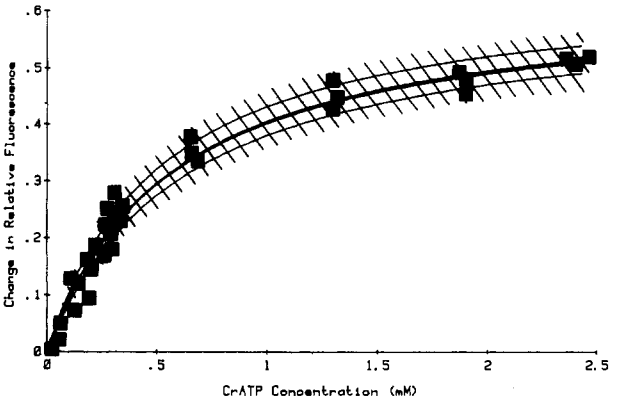

FIGURE 2: Titration of CrATP with hexokinase SII and error analysis of binding curve. Binding curve (dark, solid line) is a computer fit of the data (see text). This curve is representative of the results presented in Tables III and IV. Light, solid lines represent the standard error limits (lower curve is defined by $K_d = 0.63$ and $\Delta F_{max} = 0.62$; upper curve is defined by $K_d = 0.53$ and $\Delta F_{max} = 0.66$). The 95% confidence limits are represented by the crosshatched area.

Table IV: Effects of Metal-ATP Ligands on 2,6-TNS-Hexokinase PII Fluorescence[a]

condition	K_d (mM)	maximum change in relative fluorescence quenching[b]
MgATP	2.6 ± 0.9	0.28 ± 0.04
+50 mM lyxose	1.3 ± 0.3	0.35 ± 0.03
AlATP	no change in fluorescence	
+50 mM glucose	0.0046 ± 0.0005	0.57 ± 0.02
+50 mM lyxose	0.11 ± 0.05	0.58 ± 0.01
CrATP	0.82 ± 0.18	0.49 ± 0.04
+50 mM glucose	0.21 ± 0.02	0.66 ± 0.04

[a] 2,6-TNS fluorescence of (metal-ATP)-hexokinase binary complexes and (metal-ATP)-sugar-hexokinase ternary complexes with hexokinase PII. Values were obtained by computer fitting data to binding curves. Titrations were performed with 0.1 mg/mL hexokinase PII in 10^{-4} M 2,6-TNS and 100 mM TEA, pH 6.5. Quenching of fluorescence emission was observed at 450 nm by using an excitation wavelength of 295 nm. [b] Calculated as $(F_a - F_p)/F_a$ where F_a and F_p are the fluorescence in the absence and presence of the nucleotide, respectively.

The dissociation constant (K_d) of MgATP for binding to free enzyme was 1.7 ± 0.4 mM and was decreased by the presence of lyxose. Glucose and 5-thioglucose were not tested since these sugar ligands would have formed a productive ternary complex with hexokinase in the presence of MgATP. The K_d for citrate-treated ATP was determined to be 1.1 ± 0.1 mM. The presence of glucose, 5-thioglucose, or lyxose decreased the K_d for citrate-treated ATP binding, and *N*-acetylglucosamine had no effect. The titration of free hexokinase with AlATP was unique in that no change in 2,6-TNS fluorescence was observed; the presence of a sugar ligand was apparently required for binding this metal–ATP ligand. The glucose–hexokinase complex demonstrated the lowest K_d for AlATP. The lyxose–hexokinase complex demonstrated a significantly higher K_d value, but this value was lower than the K_d values determined for either the 5-thioglucose–hexokinase complex or the *N*-acetylglucosamine complex. The K_d for CrATP binding to free enzyme was determined to be 0.58 ± 0.5 mM. The presence of either glucose or lyxose decreased this K_d value with lyxose demonstrating the greater effect. *N*-Acetylglucosamine and 5-thioglucose slightly increased this K_d value.

Table V: Effect of Metal-ATP Ligands on Intrinsic Fluorescence of Sugar-Hexokinase PII Complexes[a]

ligand	maximum change in relative fluorescence (%)	K_d
MgATP		
+lyxose	no change	
AlATP		
+glucose	−8 ± 2	1.9 ± 2.3 μM
+lyxose	−4 ± 2	
+mannosamine	−16 ± 6	4.8 ± 2.0 μM
TbATP		
+glucose	−4 ± 1	
+lyxose	no change	
+mannosamine	no change	
citrate-treated ATP		
+glucose	−9 ± 2	0.18 ± 0.07 mM
+lyxose	−3 ± 2	
+mannosamine	−5 ± 1	

[a] Change in intrinsic fluorescence of sugar-hexokinase PII complexes upon binding metal-ATP ligands. Titrations were performed with 0.1 mg/mL hexokinase PII in 100 mM TEA, pH 6.5, at 50 mM sugar as described under Materials and Methods. K_d values were calculated from Hanes' plots. Due to problems with metal-ATP chelate solubility, titrations of two metal-ATP ligands were limited to the following maximal concentrations: AlATP, 0.1 mM; TbATP, 0.5 mM.

Several of these metal–ATP titrations were repeated with hexokinase PII (Table IV). The K_d values for metal–ATP binding to free enzyme and several of the sugar–hexokinase complexes demonstrate slight quantitative differences for this enzyme form, but the changes are qualitatively similar to those observed with hexokinase SII.

The conformational states of hexokinase in the presence of sugar and metal–ATP ligands were monitored for time-dependent changes in 2,6-TNS fluorescence. With the exception of CrATP, no changes were observed during (at least) 10 min of incubation (Ohning, 1983). The K_d values reported above for CrATP represent the formation of the initial CrATP–(sugar)–hexokinase complex. The slow changes in hexokinase-bound 2,6-TNS fluorescence observed upon addition of CrATP will be presented in another paper.

Intrinsic Tryptophan Fluorescence. Hexokinase PII was titrated (in the absence of probes) with several sugar ligands by using an excitation wavelength of 280 nm, and the intrinsic fluorescence at 330 nm was monitored by using fixed emission or spectra. Maximum quenching was attained by all sugar ligands at concentrations at or below 10 mM. Glucose demonstrated the greatest effect by causing a 12% quenching in intrinsic fluorescence at saturation. The dissociation constant for glucose binding to hexokinase was calculated as 0.35 ± 0.21 mM. The other sugar ligands, lyxose, xylose, mannosamine, and 5-thioglucose, all demonstrated a 4% quenching of hexokinase intrinsic fluorescence at saturation. These latter changes in fluorescence were not large enough to allow accurate dissociation constants to be calculated. These titrations were repeated by using an excitation wavelength of 295 nm, and similar results were obtained. The emission maximum for hexokinase fluorescence was not altered by the presence of any of these sugar ligands at 20 mM concentration.

Sugar–hexokinase complexes were titrated with metal–ATP ligands at an excitation wavelength of 295 nm to reduce the inner-cell effect correction due to the absorption of the metal–ATP ligands (Table V). Any quenching of intrinsic hexokinase fluorescence upon addition of metal–ATP ligands is in addition to the quenching effects described above for the sugar ligands. Hence, the total quenching of intrinsic fluorescence, relative to free enzyme, is the sum of the sugar ligand effect and the metal–ATP ligand effect. The lyxose–hexokinase complex was not affected by MgATP or TbATP and demonstrated small changes in fluorescence upon addition of AlATP or citrate-treated ATP, −4% and −3%, respectively. The glucose–hexokinase complex was significantly affected by AlATP, 8% quenching, and citrate-treated ATP, 9% quenching. TbATP addition resulted in a 4% quenching of intrinsic fluorescence at the highest concentration examined (500 μM), but concentrations up to 100 μM did not demonstrate any quenching of hexokinase fluorescence. Addition of 100 μM AlATP to the mannosamine–hexokinase complex resulted in a 16% quenching of intrinsic hexokinase fluorescence. Citrate-treated ATP titration resulted in a 5% quenching of intrinsic fluorescence, and TbATP had no effect on this complex. Dissociation constants, calculated from Hanes' plots, were obtained for AlATP binding to the glucose–hexokinase complex, AlATP binding to the mannosamine–hexokinase complex, and citrate-treated ATP binding to the glucose–hexokinase complex. Dissociation constants could not be calculated for the other metal–ATP conditions that were examined due to the small changes in hexokinase fluorescence observed upon addition of these ligands.

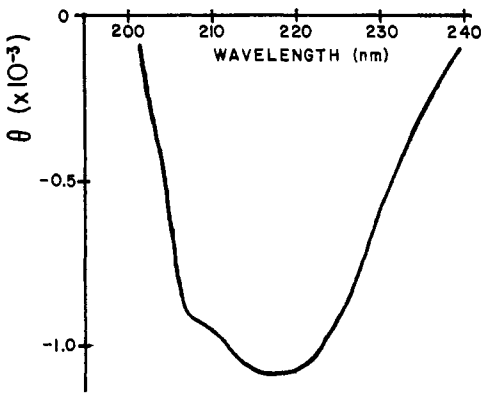

FIGURE 3: Ellipticity vs. wavelength for hexokinase SII in 100 mM TEA, pH 6.5. Ellipticity was calculated from CD spectra assuming a mean residue molecular weight of 115.

The fluorescence emission of terbium, TbATP, and the TbATP–hexokinase complex was examined by using excitation wavelengths of 260, 280, and 300 nm. Emission spectra were obtained between 450 and 650 nm, the range in which a characteristic terbium emission quartet has been demonstrated (Epstein et al., 1974). Terbium fluorescence was not altered in the formation of the TbATP chelate or the TbATP–hexokinase complex. Addition of 20 mM glucose to the TbATP–hexokinase had no effect on terbium emission.

Circular Dichroism. Circular dichroism measurements of hexokinase SII in buffer demonstrated a large negative Cotton effect in the far-UV region of the spectrum (Figure 3). This spectrum displays a wide maximum between 216–220 and a shoulder near 208 nm, indicating that hexokinase SII has a large amount of secondary structure (Simmons & Blout, 1960). The shape and position of the spectrum suggest that hexokinase contains a large amount of α-helical content and some β-structure (Greenfield & Fasman, 1969). This result is in agreement with X-ray crystallography data (Anderson et al., 1974) which indicated a high α-helical content in both lobes of the hexokinase molecule and some β-structure in one of these lobes. No significant CD spectrum was observed for hexokinase in the near-UV and visible regions. The near-UV CD spectrum was featureless with no observable signal at 0.25 mg/mL in a 1-cm cuvette, indicating an ellipticity of less than

±4.6 for the local environment of tyrosine and tryptophan in hexokinase.

The addition of 10^{-4} M 2,6-TNS or 10^{-5} M 4,4′-bis(ANS) to solutions of hexokinase SII did not alter the spectrum observed in the far-UV region, and no perturbation of enzyme ellipticity was observed in the near-UV or visible region, which indicates that binding of these probes does not significantly alter the secondary structure of hexokinase. Addition of 50 mM glucose to hexokinase, TNS–hexokinase, or ANS–hexokinase did not alter the CD spectrum in far-UV, near-UV, or visible regions. Furthermore, the addition of 50 mM lyxose or 2.1 mM CrATP to hexokinase did not alter the observed CD spectrum in any of these regions. Addition of CrATP in combination with either glucose or lyxose to hexokinase did not alter the CD spectrum in any region from that observed for the free enzyme. Similar CD results have been obtained with hexokinase PII (D. E. Clumpner and K. E. Neet, unpublished observations). Changes in hexokinase conformation induced by the binding of these ligands do not significantly alter the secondary structure of the enzyme or the symmetry of the local tyrosine or tryptophan environment. Hence, the conformational changes observed by monitoring intrinsic trypotophan fluorescence or 2,6-TNS fluorescence (described above) are apparently occurring in the random-coil regions of hexokinase. We interpret these results as the movement of the lobes of hexokinase, mediated by structural changes in the connecting region of these lobes. This "hinge" region of hexokinase has been shown to be virtually devoid of α-helix and β-structure (Steitz et al., 1977). No slow changes in the CD spectra of hexokinase or CrATP were observed.

Discussion

2,6-TNS Fluorescence and Interaction with Hexokinase. The large increase in the quantum yield and substantial blue shift of the emission maximum observed for 2,6-TNS upon binding to hexokinase suggest that this probe interacts with a hydrophobic pocket on the enzyme and/or the interaction produces a more rigid environment for the probe (Stryer, 1965). The fluorescence emission of 2,6-TNS was not significantly altered by high concentrations of KCl, and probe fluorescence was observed at pH values of 5.5, 6.5, and 8.0; therefore, ionic interactions are probably less significant in the binding of 2,6-TNS to hexokinase. Kramp & Feldman (1978) have used KI to characterize the four tryptophan residues of hexokinase as buried, partially buried, and exposed to buffer. Several lines of reasoning suggest that the bound 2,6-TNS absorbs energy from at least one tryptophan residue that is buried in a hydrophobic environment within the hexokinase molecule. (a) Emission spectra obtained with an excitation wavelength of 295 nm indicated that the intrinsic tryptophan fluorescence was significantly quenched by the binding of 2,6-TNS and that the emission maximum of the intrinsic tryptophan fluorescence underwent a 15-nm red shift in the presence of the probe. (b) An additional peak appeared in the emission spectra when an excitation wavelength of 295 nm was used corresponding to the emission maximum of 2,6-TNS at 446 nm. (c) KI had an equivalent effect on bound 2,6-TNS fluorescence at excitation wavelengths of 295 and 366 nm and was not affected by the presence of glucose. Quenching of 2,6-TNS fluorescence by KI would occur since the bound probe is exposed to buffer; however, this quenching should be independent of the excitation wavelength if the energy transfer observed at an excitation wavelength of 295 nm is due to interaction with a buried tryptophan.

Changes in the quantum yield of enzyme-bound 2,6-TNS upon addition of ligands can be due to a change in the conformation of hexokinase (resulting in an altered environment or orientation of the probe), a direct effect of the ligand on the hexokinase-bound probe molecule, or a change in the amount of probe that is bound to the enzyme. A 1:1 binding ratio was determined for 2,6-TNS and hexokinase SII, and the dissociation constant for this interaction was not altered by a variety of conditions which were shown to affect the fluorescence emission of the bound probe. The fluorescent emission of the 2,6-TNS–hexokinase PII complex was linear with protein concentration up to 0.2 mg/mL hexokinase PII. Hence, only one molecule of 2,6-TNS is bound per hexokinase monomer, and this value is not altered by the addition of sugar ligands or metal–ATP ligands. Direct effects of the various ligands on hexokinase-bound 2,6-TNS fluorescence are unlikely since both enhancement and quenching of 2,6-TNS fluorescence were observed (Lehrer, 1971). Furthermore, the presence of glucose or 5-thioglucose, two sugar ligands which caused substantial changes in hexokinase-bound 2,6-TNS fluorescence, increased the affinity of hexokinase for the metal–ATP ligands, consistent with a sugar-induced conformational change in the hexokinase molecule. X-ray crystallographic data have demonstrated that glucose binding leads to a large conformational change in the hexokinase monomer, while such a change was not observed with *o*-toluoylglucosamine (Anderson et al., 1978), in good agreement with the data presented in this paper for *N*-acetylglucosamine. The results obtained by monitoring intrinsic tryptophan fluorescence are consistent with the results obtained by examining 2,6-TNS fluorescence. Hence, the changes observed in the fluorescence properties of bound 2,6-TNS upon the addition of various ligands are interpreted as the result of changes in the conformation of the hexokinase molecule. Last, since 2,6-TNS has little or no effect on the K_m or V_{max} of hexokinase, the conformational changes in hexokinase as monitored by 2,6-TNS fluorescence are catalytically equivalent to the conformational changes of the enzyme in the absence of 2,6-TNS.

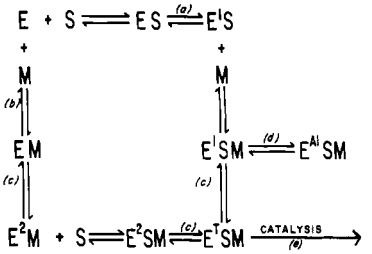

FIGURE 4: Model describing the interaction of sugar and metal–ATP with yeast hexokinase. Symbols are used to represent hexokinase (E), sugar ligands (S), and metal–ATP ligands (M). Superscripts describe different conformational states of the enzyme. Step a: If present, this step is in rapid equilibrium with the previous binding step. Step b: This step does not occur for AlATP. Step c: A more detailed model for these steps is presented elsewhere (Ohning, 1983). Step d: AlATP pathway, may be more than one step. Step e: Catalysis does not occur with citrate-treated ATP. CrATP undergoes catalysis, but release of products is very slow.

Effects of Ligand Binding on 2,6-TNS–Hexokinase Fluorescence. The six-carbon sugar ligands demonstrated varying degrees of enhancement of the bound 2,6-TNS fluorescence emission, with the good substrates, glucose, fructose, and 2-deoxyglucose, producing the largest change. These changes in 2,6-TNS fluorescence are consistent with a conformational change in hexokinase structure induced by the sugar ligands (indicated by a superscript "1" in the general binding model; Figure 4). Bennett & Steitz (1978) have correlated glucose binding with a closure of the binding cleft in the hexokinase monomer. Hence, hexokinase-bound 2,6-

TNS is sensitive to the conformational change resulting in closure of the hexokinase binding cleft. Good sugar substrates (glucose, fructose, and 2-deoxyglucose) produce a conformational state of hexokinase in which the binding cleft is closed, six-carbon sugar inhibitors (*N*-acetylglucosamine and 6-deoxyglucose) produce a conformational state in which the binding cleft is open with no effect on 2,6-TNS fluorescence, and poor sugar substrates (mannosamine and 5-thioglucose) produce an intermediate conformational state. Two models are consistent with this series of observations. First, the conformational state of hexokinase may reflect the degree to which the binding cleft is closed, i.e., different E^1 states for different hexoses (Figure 4). Therefore, all of the enzyme molecules would be in one conformation in the presence of saturating levels of a particular ligand (the equilibrium at step a would be far to the right for all hexoses). This final conformation would demonstrate maximal closure of the binding cleft in the presence of good sugar substrates and partial closure of this cleft for the other six-carbon sugar ligands, ranging from near maximal closure to little or no closure. A second, less likely, model involves nonexclusive binding of sugar to the open and closed forms in which the binding of the sugar ligand and the closure of the binding cleft are separate events. Isomerization of the enzyme–sugar complex would depend upon the specific sugar ligand that binds to the hexokinase molecule and affect the equilibrium ratio of the two forms. Hence, saturating concentrations of any sugar ligand will result in the same two conformations of the enzyme–sugar complex, one with an open binding cleft and one with a closed binding cleft, and the equilibrium distribution between these conformations will be solely dependent on the type of sugar ligand that is bound to the enzyme. The absence of time-dependent changes in bound 2,6-TNS fluorescence upon the addition of sugar ligands implies that the bimolecular and unimolecular steps of this model are in rapid equilibrium. Fluorescence (Hoggett & Kellett, 1976a,b) and temperature jump (J. E. Jentoft, J. E. Stuehr, and K. E. Neet, unpublished observations) provide further evidence that the binding of glucose and the concomitant conformational change occur rapidly.

Addition of the five-carbon sugar ligands, xylose or lyxose, resulted in a small, but significant, quenching of 2,6-TNS fluorescence, suggesting that the five-carbon inhibitors induce a smaller hexokinase conformational change that is different from the conformational change observed by the enhancement of fluorescence with the six-carbon sugar ligands. These data are in agreement with X-ray crystallographic results reported by Anderson & Steitz (1975) and Shoham & Steitz (1982). The binding of these ligands is best described by a model which is similar in form to the model presented for the six-carbon sugar ligands, except that the binding of these five-carbon sugar ligands would necessarily induce a different final conformation of the enzyme.

Binding of the good sugar substrate, glucose, to hexokinase results in an increased ability of the enzyme to bind metal–ATP ligands (Tables III and IV), but this was not observed for the poor sugar substrate, 5-thioglucose, which also gave a lower maximal fluorescent change (Table II). These data are consistent with kinetic studies reported by Viola et al. (1982) in which substrate synergism between sugar substrates and MgATP was described. The enhanced ability of most sugar–hexokinase complexes to bind metal–ATP ligands confirm that binding of metal–ATP ligands to free enzyme is not the favored pathway of ligand addition (Figure 4).

The binding of metal–ATP ligands to sugar–hexokinase complexes and free enzyme provides additional information about the conformational states induced by the sugar ligands (from the metal–ATP dissociation constants) as well as information on the qualitative effect of the metal–ATP ligands themselves on hexokinase conformational states (from the further change in 2,6-TNS fluorescence). Since the binding of metal–ATP ligands to either sugar–hexokinase complexes or free enzyme produced a quenching of the bound 2,6-TNS fluorescence, the conformational states induced by these ligands are qualitatively different from those observed upon binding of the sugar ligands. Furthermore, the presence of certain sugar ligands resulted in a significant decrease in the dissociation constants for the metal–ATP ligands. These data are analyzed in terms of changes in free energy of the sugar–hexokinase complexes relative to free, unbound hexokinase (Table VI) and the general binding scheme (Figure 4).

Table VI: Effect of Sugar Ligands on ΔG° of Metal-ATP Ligands[a]

	change in ΔG° (kcal/mol)			
	MgATP	free ATP	AlATP[b]	CrATP
glucose		0.61	3.1	0.35
lyxose	0.80	0.65	2.6	1.2
5-thioglucose		0.43	1.9	–0.30
N-acetylglucosamine	–0.20	–0.10	1.9	–0.32

[a] Change in ΔG° of metal-ATP ligands binding to hexokinase induced by the presence of sugar ligands. The difference in ΔG° for binding of metal-ATP ligands is compared for each sugar–hexokinase complex, relative to free enzyme. ΔG° values of binding were calculated from the K_d values determined by fluorescence titration (Table V). [b] For comparison only, the K_d for AlATP binding to free enzyme was assumed to be 1 mM, which would give the estimated lower limit for differences in ΔG° induced by sugar ligands for AlATP binding.

The lyxose–hexokinase complex demonstrated a significantly stronger interaction for MgATP compared to free enzyme (0.8 kcal/mol), consistent with the reported lyxose-induced enhancement of the ATPase activity for hexokinase (Rudolph & Fromm, 1971a). *N*-Acetylglucosamine had no effect on this K_d value, which is consistent with this ligand being a competitive inhibitor vs. glucose (Kaji & Colowick, 1965) without affecting the ADP–ATP exchange rate for the enzyme (Solomon & Rose, 1971). The K_d for citrate-treated ATP was decreased by the presence of glucose, lyxose, or 5-thioglucose. Glucose and lyxose had virtually identical effects on this interaction (0.61–0.65 kcal/mol), indicating that the conformational states induced by binding of these sugars are similar with respect to free ATP binding. On the other hand, the binding of CrATP to hexokinase was slightly enhanced by the presence of glucose and strongly enhanced by lyxose. The lyxose–hexokinase complex displayed a significantly lower K_d for CrATP than any of the other sugar–hexokinase complexes, in apparent contrast to the results obtained from the AlATP titrations in which glucose was observed to have the greatest effect on the K_d of AlATP. Thus, the results obtained with AlATP and CrATP support the evidence from the fluorescent properties of the sugar–hexokinase complexes that the conformational state of the glucose–hexokinase complex is different from the conformational state of the lyxose–hexokinase complex; the difference in the structure of AlATP and CrATP can distinguish between these two sugar–hexokinase conformations. *N*-Acetylglucosamine and 5-thioglucose, on the other hand, have a different effect than either glucose or lyxose with respect to these two metal–nucleotides; both slightly inhibit CrATP binding and enhance AlATP binding, but not as strongly as lyxose. The effect on metal-free ATP distinguishes the states induced by *N*-acetylglucosamine and 5-thioglucose.

MgATP, citrate-treated ATP, and CrATP demonstrated binding to free hexokinase. The similarity of the dissociation constants for MgATP and citrate-treated ATP suggests that the magnesium ion is not important in the binding of ATP to free enzyme (Table III). Addition of AlATP to free hexokinase did not alter the fluorescence emission of bound 2,6-TNS. Due to the problems with solubility of AlATP, the highest concentration of this ligand that could be tested was 100 μM; however, this was well above the steady-state inhibition constant of 0.16 μM (Viola et al., 1980; Neet et al., 1982). If AlATP bound to free hexokinase, a quenching of the 2,6-TNS fluorescence emission would be expected since the binding of this ligand to the sugar–hexokinase complexes resulted in a substantial quenching of this fluorescence. Therefore, these data provide physical, thermodynamic evidence that AlATP does not bind to free hexokinase with a K_d of less than 2 mM. Kinetic studies have shown that AlATP is a competitive inhibitor vs. MgATP and an uncompetitive inhibitor vs. glucose, which also suggests that AlATP binds in a kinetically significant fashion to the glucose–hexokinase complex but not to free enzyme (Viola et al., 1980; Neet et al., 1982). The inability of AlATP to bind to free hexokinase is in striking contrast to the K_d values obtained for the titration of this metal–ATP with the sugar–hexokinase complexes. All of these complexes were able to bind AlATP well, with glucose demonstrating a markedly low K_d compared to the other sugar–hexokinase complexes. The binding of AlATP to the *N*-acetylglucosamine–hexokinase complex is particularly interesting in that this complex had not demonstrated an increased ability to bind any of the other metal–ATP ligands. This result indicates that subtle conformational changes in hexokinase structure occur upon binding of *N*-acetylglucosamine; however, kinetic data show that these changes do not allow for the formation of a productive ternary complex and the similar compound, *o*-toluoylglucosamine does not allow cleft closure.

The binding of AlATP to free hexokinase was not observed at the highest measurable concentration of this ligand (100 μM) whereas CrATP did with a K_d of 0.58 mM. The slow changes in 2,6-TNS fluorescence observed in the presence of CrATP were not observed with AlATP (Ohning, 1983). Thus the conformational states initially induced by these two metal–ATP ligands appear to be different. CrATP has been reported to be a substrate for the hexokinase phosphorylation reaction; however, it acts as a dead-end inhibitor due to the slow release of the products of this reaction. Conversely, AlATP has not been demonstrated to act as a phosphate donor in the hexokinase reaction. Since these metal–ATP ligands demonstrate differences in their ability to undergo phosphate transfer in the hexokinase transition state complex, it is not suprising that different conformational states are induced by these ligands.

Our current understanding of the conformational states of the hexokinase monomer may be summarized as follows (Figure 4). Various sugars bind in rapid equilibrium with differing degrees of cleft closure (isomerization a) and corresponding differing abilities to promote metal–nucleotide binding. ATP, MgATP, and CrATP can bind to free enzyme (steps b and c, left side) to form a conformationally different enzyme form, E^2, with 2,6-TNS fluorescence; CrATP undergoes the isomerization EM to E^2M slowly (Ohning, 1983). In the presence of good substrates (glucose) the nucleotides bind thermodynamically (this study) and kinetically (Noat et al., 1969; Wilkinson & Rose, 1979; Danenberg & Cleland, 1975) preferentially to the E^1S form. AlATP forms a dead-end complex (isomerization d) which does not undergo catalysis and is apparently different from the E^TSM active complex conformation formed by productive complexes. Evidence for the ternary conformational state E^TSM is provided by further fluorescence changes to form the complexes glucose–ATP–hexokinase, lyxose–MgATP–hexokinase, and glucose–CrATP–hexokinase; only the latter occurs slowly. Differences in fluorescence of the 2,6-TNS ternary complexes suggest different E^TSM conformational states with different ligand pairs.

Registry No. 2,6-TNS, 7724-15-4; ATP, 56-65-5; glucose, 50-99-7; fructose, 57-48-7; 2-deoxyglucose, 154-17-6; 5-thioglucose, 20408-97-3; mannosamine, 2636-92-2; *N*-acetylglucosamine, 7512-17-6; 6-deoxyglucose, 7658-08-4; lyxose, 65-42-9; xylose, 58-86-6; MgATP, 1476-84-2; AlATP, 74078-60-7; CrATP, 69381-95-9; TbATP, 74078-68-5; hexokinase, 9001-51-8.

References

Adler, A., Greenfield, N., & Fasman, G. (1973) *Methods Enzymol. 27*, 675–735.

Anderson, C. M., Steinkamp, R. E., McDonald, R. C., & Steitz, T. A. (1978) *J. Mol. Biol. 123*, 207–219.

Anderson, W. F., & Steitz, T. A. (1975) *J. Mol. Biol. 92*, 279–287.

Anderson, W. F., Fletterick, R. J., & Steitz, T. A. (1974) *J. Mol. Biol. 86*, 261–269.

Bennett, W. S., & Steitz, T. A. (1978) *Proc. Natl. Acad. Sci. U.S.A. 75*, 4848–4852.

Brand, L., & Witholt, B. (1967) *Methods Enzymol. 11*, 776–856.

Cavalieri, R. L., & Sable, H. Z. (1974) *Anal. Biochem. 59*, 122–128.

Chen, R., Edelhoch, H., & Steiner, R. (1969) *Physical Principles and Techniques of Protein Chemistry* (Leach, S. J. Ed.) Part A, Chapter 4, pp 171–244, Academic Press, New York.

Colowick, S. P. (1973) *Enzymes, 3rd Ed. 9*, 1–48.

Danenberg, K. D., & Cleland, W. W. (1975) *Biochemistry 14*, 28–39.

De Domenech, E. E. M., & Sols, A. (1980) *FEBS Lett. 119*, 174–176.

De Pamphilis, M. L., & Cleland, W. W. (1973) *Biochemistry 12*, 3714–3724.

Epstein, M., Levitzki, A., & Reuben, J. (1974) *Biochemistry 13*, 1777–1782.

Feldman, I., & Kramp, D. C. (1978) *Biochemistry 17*, 1541–1547.

Fromm, H. J., & Zewe, V. (1962) *J. Biol. Chem. 237*, 3027–3032.

Greenfield, N., & Fasman, G. (1969) *Biochemistry 8*, 4108–4116.

Hoggett, J. G., & Kellett, G. L. (1976a) *Eur. J. Biochem. 66*, 65–77.

Hoggett, J. G., & Kellett, G. L. (1976b) *Eur. J. Biochem. 68*, 347–353.

Holroyde, M., Chester, J., Trayer, I., & Walker, D. (1976) *Biochem. J. 153*, 351–361.

Job, P. (1928) *Justis Liebigs Ann. Chem. 9*, 113–203.

Kramp, D. C., & Feldman, I. (1978) *Biochim. Biophys. Acta 537*, 406–416.

Kaji, A., & Colowick, S. P. (1965) *J. Biol. Chem. 240*, 4454–4462.

Lehrer, S. S. (1971) *Biochemistry 10*, 3254–3263.

Mayer, E. L., Hoggett, J. G., & Kellett, G. L. (1982) *Biochem. J. 203*, 523–525.

McClure, W. O., & Edelman, G. M. (1966) *Biochemistry 5*, 1908–1919.
McDonald, R. C., Steitz, T. A., & Engelman, D. M. (1979) *Biochemistry 18*, 338–342.
Neet, K. E., Furman, T. C., & Hueston, W. J. (1982) *Arch. Biochem. Biophys. 213*, 14–25.
Noat, G., Richard, J., Borel, M., & Got, C. (1969) *Eur. J. Biochem. 11*, 106–112.
Ohning, G. V. (1983) Ph.D. Dissertation, Case Western Reserve University.
Peters, B. A., & Neet, K. E. (1978) *J. Biol. Chem. 253*, 6826–6831.
Rudolph, F. B., & Fromm, H. J. (1971a) *J. Biol. Chem. 246*, 2104–2110.
Rudolph, F. B., & Fromm, H. J. (1971b) *J. Biol. Chem. 246*, 6611–6619.
Rustum, A. H., Ramel, Y. M., & Barnard, E. A. (1971) *Prep. Biochem. 1*, 309–329.
Schmidt, J. J., & Colowick, S. P. (1973) *Arch. Biochem. Biophys. 158*, 417–477.
Schulze, I. T., & Colowick, S. P. (1969) *J. Biol. Chem. 244*, 2306–2316.
Shoham, M., & Steitz, T. A. (1982) *Biochim. Biophys. Acta 705*, 380–384.
Simmons, N., & Blout, E. (1960) *Biophys. J. 1*, 55–62.
Solomon, F., & Rose, I. A. (1971) *Arch. Biochem. Biophys. 147*, 349–350.
Steitz, T. A., Anderson, W. F., Fletterick, R. J., & Anderson, C. M. (1977) *J. Biol. Chem. 252*, 4494–4500.
Stryer, L. (1965) *J. Mol. Biol. 13*, 482–495.
Viola, R. E., Morrison, J. F., & Cleland, W. W. (1980) *Biochemistry 19*, 3131–3137.
Viola, R. E., Rauschel, F. M., Rendina, A. R., & Cleland, W. W. (1982) *Biochemistry 21*, 1295–1302.
Wilkinson, K. D., & Rose, I. A. (1979) *J. Biol. Chem. 254*, 12567–12572.
Womack, F. C., & Colowick, S. P. (1979) *Proc. Natl. Acad. Sci. U.S.A. 76*, 5080–5084.
Zewe, V., Fromm, H. J., & Fabiano, R. (1964) *J. Biol. Chem. 239*, 1625–1634.

Fluorescent Properties of Pyrene Bound at Specific Acylation Sites of Chicken Liver Fatty Acid Synthase†

Vernon E. Anderson‡ and Gordon G. Hammes*

ABSTRACT: The covalent modification of chicken liver fatty acid synthase by 4-(1-pyrenyl)butyryl-CoA (PBA-CoA), a fluorescent analogue of acetyl- and malonyl-CoA, has been studied. The binding isotherms and the kinetics of inactivation suggest 2 mol of PBA-CoA/mol of enzyme is specifically incorporated into the enzyme. Two classes of binding sites have been identified by determining the fluorescence lifetimes of enzyme-bound pyrene, by the quenching of enzyme-bound pyrene fluorescence with iodide, and by neutral hydroxaminolysis of both the native and denatured PBA-CoA-modified enzymes. Hydroxaminolysis of the denatured enzyme indicates that 4-(1-pyrenyl)butyric acid is esterified to both hydroxyl and thiol groups. The portion esterified to the hydroxyl is readily removed from the native enzyme by treatment with neutral hydroxylamine, indicating that the oxygen ester is unstable to hydroxylamine in the native enzyme. Iodide and acrylamide quenching of the enzyme-bound pyrene fluorescence shows that solvent access to both classes of pyrene binding sites is restricted. Iodide preferentially quenches one class of sites in the native enzyme, but these sites are not differentiated in the monomeric or denatured enzyme. The steady-state anisotropy, 0.083, indicates the enzyme-bound pyrene has considerable rotational freedom. The dynamic anisotropy can be characterized solely by a viscosity-dependent rotational correlation time of 610 ns, which is ascribed to the rotational motion of the dimeric enzyme.

Animal fatty acid synthases are multienzyme complexes that catalyze the synthesis of palmitate from acetyl-CoA,[1] malonyl-CoA, and NADPH. The reaction proceeds through a cycle of seven condensations of an enzyme-bound malonyl moiety with the growing enzyme-bound saturated fatty acid chain. Each condensation is followed by reduction of the β-keto intermediate, dehydration of the alcohol, and reduction of the carbon–carbon double bond formed. The acylation sites on the enzyme complex have been postulated to be 4′-phosphopantetheine, a cysteine, and a serine or threonine (Jacob et al., 1968; Chesterton et al., 1968; Phillips et al., 1970a,b). The cysteine and 4′-phosphopantetheine sites have been proposed as common sites for acetyl and malonyl residues in all eukaryotic fatty acid synthases (Stoops & Wakil, 1981). The hydroxyl site is probably a loading site, and the 4′-phosphopantetheine serves to transfer the intermediate states of the growing fatty acid chain to the various catalytic sites of the enyzme.

The nature of the acylation reaction has been previously investigated with a fluorescent CoA derivative (Cardon & Hammes, 1982, 1983) and with acetyl-CoA (Cognet & Hammes, 1983). The fluorescent CoA derivative previously used, NBD-CoA,[1] was selected because the relatively small size of the fluorophore confers binding properties on the CoA derivative which appear to be similar to those of substrates,

† From the Department of Chemistry, Cornell University, Ithaca, New York 14853. *Received December 17, 1982.* This work was supported by grants from the National Institutes of Health (GM 13292) and National Science Foundation (PCM 8120818).
‡ National Institutes of Health Postdoctoral Fellow (GM 9047).

[1] Abbreviations: PBA, 4-(1-pyrenyl)butanoic acid; CoA, coenzyme A; EDTA, ethylenediaminetetraacetic acid; NBD, 7-chloro-4-nitro-2,1,3-benzoxadiazole.

0006-2960/83/0422-2995$01.50/0